Estimation of spectral shifts of fluorinated liquid crystals in ultraviolet region: Role of correlations in molecular structures

T. JAISON JOSE[a], A. SIMI[b], M. DAVID RAJU[c], P. LAKSHMI PRAVEEN[d]
[a]P. G. Department of Chemistry, Andhra Loyola College, Vijayawada-520 008,Andhra Pradesh, India
[b]Department of Chemistry, St. Joseph's College, Tiruchirapalli-620 002,Tamil Nadu, India
[c]P. G. Department of Chemistry, P. B. Siddhartha College of Arts & Sciences, Vijayawada-520 010, Andhra Pradesh, India
[d]Department of Physics, Veer Surendra Sai University of Technology, Burla-768 018, Odisha, India

Estimation of spectral shifts of a series of alkyl 4-[2-(perfluorohexyl) ethoxy] benzoates (*n*PFHEB) have been studied by varying the number of carbon atoms (*n*) in alkyl chain with *n*=5, 6, and 9 in ultraviolet (UV) region. Structure of these molecules have been optimized using the Density functional B3LYP with 6-31+G (d) basis set using crystallographic geometry as input. The spectral shifts of these molecules have been estimated in the UV region by employing the DFT method, semiempirical CNDO/S and INDO/S parameterizations. The oscillator strength (*f*) and vertical transition energy (E_V) have been reported corresponding to absorption wavelength (λ_{max}). The UV absorption behaviour and stability of the molecules have been discussed based on the reported data. These results indicate that the alkyl chain length and correlations in molecular structures may be used for tuning the electronic and optical properties of the molecules.

1. Introduction

Liquid crystals (LCs) are extensively used as anisotropic materials that have self-organizing properties. The physical features of LCs can be altered with introduction of a fluorine atom or fluorinated group. However, much literature has not been cited about fluorinated LCs in spite of their potential applications [1, 2]. Compounds with highly fluorinated alkyl chains have been used as structural units in the construction of self-assembled architectures. Fluorination of LCs has a significant effect on properties, and it leads to the supremacy of smectic phases [3, 4]. One fascinating aspect of highly fluorinated alkyl chains is that they allow even a single aromatic ring compounds to exhibit LC phases [5, 6]. This may be helpful for designing of new LCs with structural flexibility.

Photo-induced phenomenon, in which incident light causes molecular ordering/ disordering of LC system has been emerged as new dimension. This photo-induced optical anisotropy offers future potential technology for optical storage devices. In many opto-electronic applications using LC devices, light absorption has become an important issue depending on the wavelength region of interest. For instance, to steer a high power laser beam or to produce quality images by employing a high power lamp, the absorbed light is converted to thermal energy. Consequently, this heats up the LC cell. Since, the physical properties of a thermotropic LC are sensitive to the temperature; the performance of the LC device will be affected through the absorption of light [7, 8].

The absorption of a LC compound in UV spectral regions, and the electronic transitions are helpful in analyzing the UV stability of LC molecules. The $\sigma \rightarrow \sigma^*$ electronic transitions take place in the vacuum UV (100–180nm) region, whereas, the $\pi \rightarrow \pi^*$ electronic transitions occur in the UV (180–400nm) region. The UV absorption affects the photo stability, and lifetime of a LC device. A high energy UV photon may break the chemical bond of a long chain LC molecule, and cause deterioration in molecular alignment which, in turn, degrades the device performance. The major optical loss originates from light scattering due to the LC director fluctuations, rather than absorption. The end user demand for larger screens that have ever sharper image quality continues to drive modernization in the design and application of novel LC materials that can deliver higher performance display systems. Commercial LC mixtures generally consist of 10–15 molecular components, each of which contributes to the overall performance of the LC display image. In view of this, high demand persists for mono component LCs with high stability in UV and visible regions. Further, from a theoretical point of view, most previous works focus mainly on the central (core) part of the molecules, as it is responsible for the π-π stacking, and for the electronic structure of the material. This is due to the usual assumption that both Highest Occupied Molecular Orbital (HOMO) and Lowest Unoccupied Molecular Orbital (LUMO) energy levels are located in core part of the

molecule. Therefore, the present study has been focused towards the estimation of spectral shifts of *n*PFHEB (*n*=5, 6, 9) molecules by maintain the common core, and side groups. The alkyl chain length dependence and correlation in molecular structures have been discussed.

The estimation of spectral shifts is particularly interesting, since number of methods have been employed to calculate the absorption wavelengths, and oscillator strengths of electronic transitions. The methods based on Time Dependent Density Functional Theory (TDDFT) applied to small and middle sized systems provide rather good accuracy at low computational cost [9]. Further, it is well known that DFT-based methods have limits to treat organic molecules [10], and for establishing realistic molecular models. Hence, the alternate use of semiempirical schemes has an extensive use to estimate spectral shifts in the desired wavelength regions. Such approaches allow for the calculation of electronic transitions between the ground state and the different excited states, which gives the energies of the corresponding radiations. The present study aims at providing a comparative picture of *n*PFHEB (*n*=5, 6, 9) molecules using semiempirical CNDO/S (complete neglect of differential overlap/ spectroscopy) [11, 12], INDO/S (intermediate neglect of differential overlap/ spectroscopy) [13-15] schemes and DFT method. It concentrates on the alkyl chain length dependence, and correlation in molecular structures. The HOMO, LUMO energies, oscillator strength (*f*) have also been reported. An examination of thermodynamic data has revealed that *n*PFHEB molecules exhibits smectic B-isotropic transition temperature as follows [16]: 5PFHEB at 340.7K; 6PFHEB at 332K; and 9PFHEB at 327.4K.

2. Liquid crystal models and computational methods

The present study adopts three methods for the estimation of spectral shifts of *n*PFHEB (*n*=5, 6, 9) molecules namely DFT, CNDO/S, and INDO/S. An efficient and widely used technique to study a molecular structure is DFT [17]. This method with B3LYP/6-31+G(d) level of calculation has been applied to optimise the *n*PFHEB molecules in the gas phase. The B3LYP (Becke–Lee–Yang–Parr) version of DFT is the combination of Becke's three parameter non-local hybrid functional of exchange terms with the Lee, Yang and Parr correlation functional. The basis set of 6–31+G (d) contains a reasonable number of basis set functions. The geometry optimizations have been performed using the density functional theory (DFT) approach without symmetry constraints.

The DFT approach was originally developed by Hohenberg and Kohn [18], Kohn and Sham [19, 20] to provide an efficient method of handling many-electron system. For singlet ground states, DFT calculations have performed using the B3LYP functional. For singlet excited states, the excitation energies and oscillator strengths at the optimised geometry in the ground state have been obtained by TDDFT calculations with the B3LYP functional coupled with the configuration interaction (CI) single level of approximation including all $\pi\rightarrow\pi^*$ single excitations. This has been found adequate to determine the UV-Visible absorption spectra [21, 22] provided that suitable parameterizations are used.

For the $\pi\rightarrow\pi^*$ state a considerable theoretical literature exists, but there is still uncertainty about the precise position of the vertical transition. Hence, a database has to be formulated in terms of vertical transition energies corresponding to $\pi\rightarrow\pi^*$ transitions. In the present work, a comparative analysis has been carried out by employing CNDO/S, INDO/S, and DFT methods to estimate the spectral shifts of the investigated molecules in UV region. The DFT calculations have been performed by a spectroscopy oriented configuration interaction procedure (SORCI) [23], whereas, a revised version of QCPE 174 by Jeff Reimers, University of Sydney and co-workers have been used for the semiempirical calculations [24]. Furthermore, using the results obtained from the calculation, the structural and electronic properties such as HOMO (H), LUMO (L) energies, energy gap ($E_g=E_L-E_H$), ionzsation energy (I), electron affinity (A), electro negativity (χ), chemical hardness (η), electronic chemical potential (μ), electrophilicity index (ω), and softness (S) have been investigated. The general structural parameters of the systems such as bond lengths, and bond angles have been taken from published crystallographic data [16].

3. Results and discussion

Structures of smectogenic alkyl 4-[2-(perfluorohexyl) ethoxy] benzoates (*n*PFHEB) with various alkyl chain carbon atoms (*n*=5, 6, 9) have been optimized using Density functional B3LYP with 6-31+G (d) basis set using crystallographic geometry as input. Using the optimized geometry, structure of the molecules has been evaluated using the DFT calculations. The chemical structure of *n*PFHEB molecules, and the DFT optimized molecular structures have been shown in Fig. 1. Much of the interesting phenomenology of liquid crystals involves the geometry and dynamics of the structure. Hence, Fig. 1 is essential to understand and design of the new molecules. The group charges of the molecules using Mulliken, Loewdin population analysis have been reported in Table 1. The molecular charge distribution, and phase stability of the compounds have been analyzed as given below:
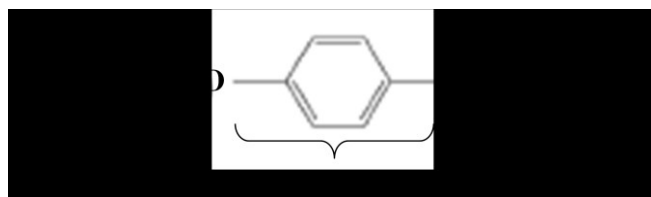
n=5, 5PFHEB; *n*=6, 6PFHEB; *n*=9, 9PFHEB; *m*=6

(a)

(b)

(c)
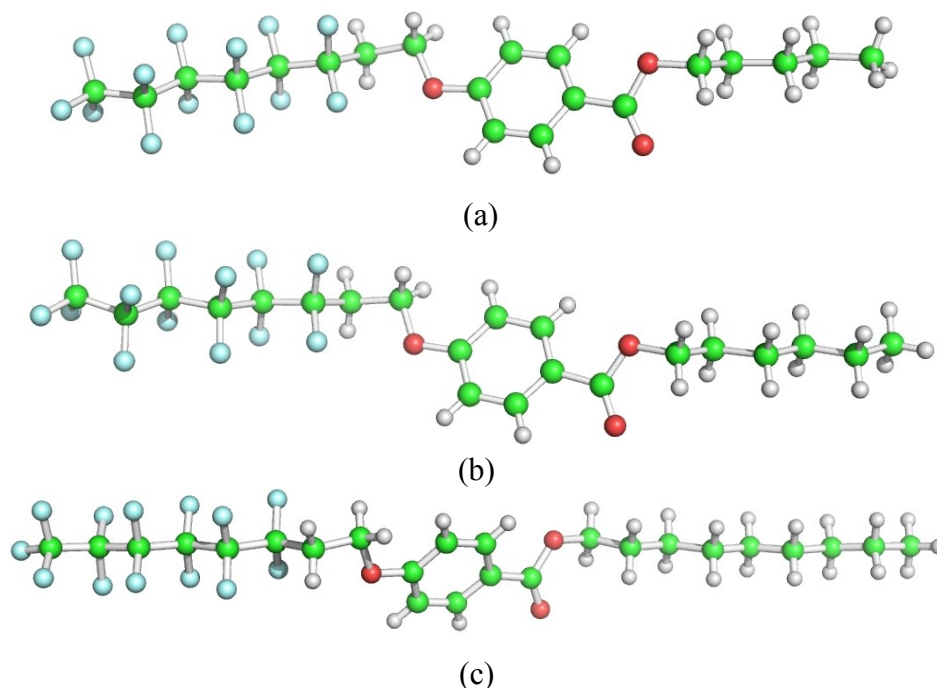
Fig. 1. Molecular geometry of nPFHEB (n=5, 6, 9) molecules

*Table 1. Mulliken (M) and Loewdin (L) group charges and smectic B-isotropic transition temperatures
for nPFHEB (n=5,6, 9) molecules*

Molecule	Side Group		Core		End Group		T_{S-I}/K
	M	L	M	L	M	L	[16]
5PFHEB	-4.70	-3.60	5.15	3.90	-0.45	-0.29	340.7
6PFHEB	-4.67	-3.60	5.12	3.89	-0.45	-0.28	332
9PFHEB	-4.75	-3.63	5.19	3.92	-0.44	-0.28	327.4

3.1. Molecular charge distribution and phase stability

The reactivity of a molecule may be inferred from its electron density distribution. One way to quantify such a distribution is by means of a charge population analysis. The charge at each atomic centre is assigned by the sum of its nuclear charge (atomic number) and the number of electrons occupying the orbitals belonging to that atom. An appropriate modeling of mesophases relies on the possibility of assigning a partial charge to all atomic centers. The atom positioned partial charges are helpful to parameterize the molecular interactions for computational studies. Quantum chemical computations offer the possibility to take a detailed look at the electronic structure of the molecules. This can be done, by determining atom-based partial charges, which are not quantum mechanical observables.

The group charges are needed to explain the phase stability, and the details of transition temperatures of mesogens. Computed Mulliken, and Loewdin group charges have been reported in Table 1. These group charges have been compared to establish the correlation between molecular charge distribution, and phase stability of the molecules. The aromatic rings along with the oxygen atoms have been considered as core. The left and

the right sides of the core have been taken as side, and end groups in the calculation (Fig. 1). Much agreement among the methods has been found in terms of the group charges on each molecule. The results show that the core structure plays a vital role on charge distribution, and phase stability. Evidently, the core in 5PFHEB molecule consists of a positive charge. Hence it will be strongly attracted by the both side, and end negative charge groups causing the strong binding in the phase transition. Hence, the phase stability has been expected to be high for 5PFHEB. Further, the thermal vibration amplitude of the chain carbon atoms increase markedly with the increase of chain length, indicating a low packing efficiency for higher homologues. This leads to the drastic decrease in phase stability. This is in agreement with the smectic B-isotropic transition temperature reported by the crystallographer (Table 1).

3.2. UV-visible absorption spectrum

The UV spectra of molecules are associated with the electronic transitions involving π and/or n electron systems. The molecules containing aromatic groups have strong absorptions in the UV regions. The interaction of light with LC molecules is of essential interest in order to gain insight into its electronic structure, and to design new optical devices. The analysis of elementary charge, excitation energy transfer steps in small and high absorption LCs require quantum chemical methodology. These elementary processes determine the applicability of such systems in flexible displays, and photovoltaic devices. This provides an explanation of the sequential process to effect the photo sensitivity, and response time of the designed molecules.

LCs are model materials for such applications as they are especially sensitive to electrical fields, exhibit short response times on the submicron scale, and feature excellent transparency over a broad spectral range, from ultraviolet to visible to infrared. The addition of substituent atoms is the widely used technique in order to change the physical properties of LC molecules. In the calculation of electronic spectra, the configuration interaction (CI) method is widely employed. Using a CI method in combination with a semi-empirical model Hamiltonian, an evaluation of absorption spectra of large organic molecules and LCs becomes possible [25]. The analysis of UV-Visible absorption spectra of nPFHEB (n=5, 6, 9) molecules based on DFT data (Fig. 2) has been given below. Further, Fig. 3, 4 represents the UV spectra of these molecules based on CNDO/S, and INDO/S methods respectively.
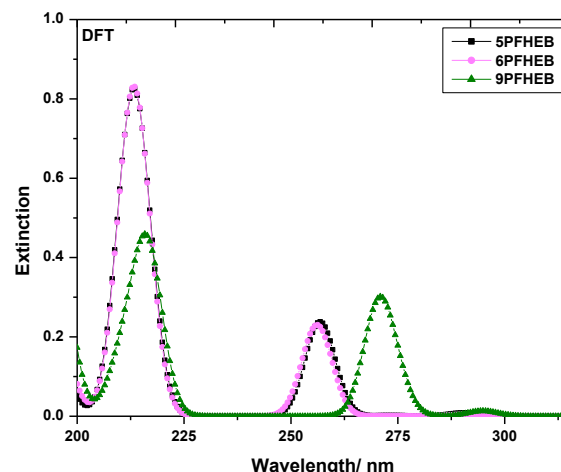
Fig. 2. UV absorption spectra of nPFHEB molecules using DFT method
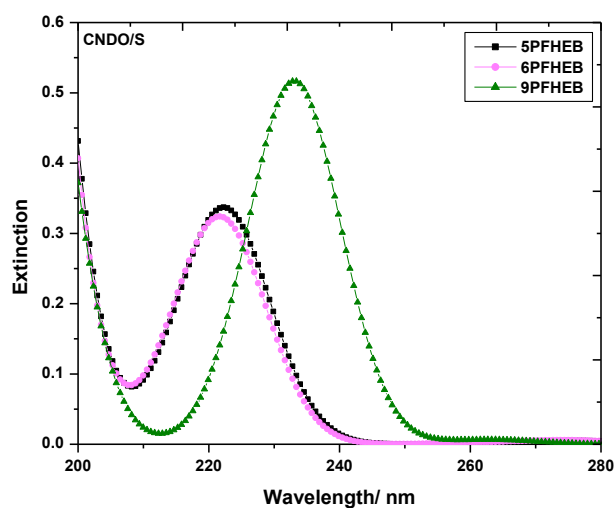
Fig. 3 UV absorption spectra of nPFHEB molecules using CNDO/S method
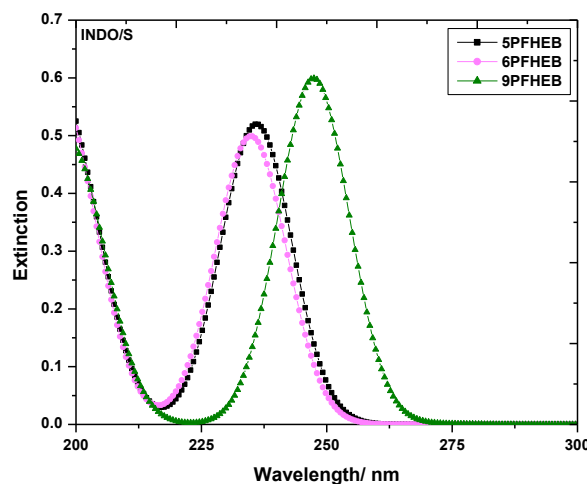
Fig. 4. UV absorption spectra of nPFHEB molecules using INDO/S method

5PFHEB The UV absorption spectrum of 5PFHEB molecule has been shown in Fig. 2 using DFT method. A three-band structure has been observed in the UV region with absorptions at 213.48nm (λ_1), 256.84nm (λ_2), and 290.23nm (λ_3) (not so clear in the figure). However, no absorption has been observed in the visible region. The strongest band appears in a region of 202.93nm to 225.20nm with absorption maxima (λ_{max}) at 213.48nm. This band arises from the HOMO→LUMO transition, and is assigned as $\pi \to \pi^*$ transition in the molecule. The other absorption bands corresponding to the remaining wavelengths in UV region also indicate the possibility of $\pi \to \pi^*$ transitions in the molecule at higher wavelengths. The oscillator strengths (f) of these three absorptions corresponding to λ_1, λ_2, and λ_3 are 0.40, 0.24, and 0.01 respectively. Therefore, these transitions contribute the highest oscillator strength corresponding to absorption band at λ_1.

6PFHEB The UV absorption spectrum of 6PFHEB molecule has been shown in Fig. 2 using DFT method. A three-band structure has been observed in the UV region with absorptions at 213.47nm (λ_1), 256.25nm (λ_2), and 290.82nm (λ_3) (not so clear in the figure). However, no absorption has been observed in the visible region. The strongest band appears in a region of 202.93nm to 224.61nm with absorption maxima (λ_{max}) at 213.48nm. This band arises from the HOMO→LUMO transition, and is assigned as $\pi \to \pi^*$ transition in the molecule. The other absorption bands corresponding to the remaining wavelengths in UV region also indicate the possibility of $\pi \to \pi^*$ transitions in the molecule at higher wavelengths. The oscillator strengths (f) of these three absorptions corresponding to λ_1, λ_2, and λ_3 are 0.39, 0.23, and 0.004 respectively. Therefore, these transitions contribute the highest oscillator strength corresponding to absorption band at λ_1.

9PFHEB The UV absorption spectrum of 9PFHEB molecule has been shown in Fig. 2 using DFT method. A three-band structure has been observed in the UV region with absorptions at 215.82nm (λ_1), 270.90nm (λ_2), and 294.92nm (λ_3). However, no absorption has been observed in the visible region. The strongest band appears in a region of 204.69nm to 226.95nm with absorption maxima (λ_{max}) at 215.82nm. This band arises from the HOMO→LUMO transition, and is assigned as $\pi \to \pi^*$ transition in the molecule. The other absorption bands corresponding to the remaining wavelengths in UV region also indicate the possibility of $\pi \to \pi^*$ transitions in the molecule at higher wavelengths. The oscillator strengths (f) of these three absorptions corresponding to λ_1, λ_2, and λ_3 are 0.42, 0.26, and 0.01 respectively. Therefore, these transitions contribute the highest oscillator strength corresponding to absorption band at λ_1.

3.3. Alkyl chain length dependence

The DFT data shows that 5PFHEB molecule exhibits absorption maxima (λ_{max}) at 213.48nm, 6PFHEB at 213.47nm, and 9PFHEB at 215.82nm. Thus, the substitution of one alkyl group in 5PFHEB (forming 6PFHEB) leads to a blue-shift (the shift of absorption maxima to a lower wavelength), whereas, four alkyl groups (forming 9PFHEB) leads to a red-shift. The increment in alkyl chain length causes the planarization of 9PFHEB molecule (Fig. 1) is responsible for the red-shift. Further, this also causes the hypochromic effect (decrement in absorbance) in both cases. A comparative picture of the absorption bands, corresponding extinction coefficients (EC), vertical excited energy (E_V), oscillator strength (f), HOMO, LUMO, and energy gap values using the DFT, CNDO/S, and INDO/S methods have been reported in Table 2, 3, 4 respectively.

It is evident that the substitution of additional alkyl groups has a significant effect on the spectral parameters. The induced blue/red-shifts of absorption wavelength cause an increment/decrement in excited energies. This ultimately, affects the other spectral parameters. The HOMO, LUMO and energy gap values have been reported. A very good agreement has been noticed among all the methods in estimating the absorption maxima of these compounds. The excitation of the electron makes the band to weak electrostatic interaction, due to which the absorbing wavelength at lower wavelength side may be observed. This indicates a strong exciton coupling of chromophores. The high phase stability of 5PFHEB molecule (section 3.1) makes the band to interact less electrostatically, leads to a change in charge distribution, and a decreased delocalization of electrons. Thus, both the ground, and excited $n \to \pi^*$ transition do not occur due to the lack of rigidity in the ring system of the molecules. The comparison of absorption maxima values indicates that 9PFHEB exhibits a higher value at longer wavelength. This indicates that the high photo sensitivity of 9PFHEB. Further, it also causes lower band gap compared to other two molecules. Hence, the conductivity is high for 9PFHEB molecule. These significant aspects of organic fluorinated liquid crystals with appreciably modified properties with respect to mesophase morphology, transition temperatures, optical, electric and visco-elastic properties in terms of fundamental structure-property relationships is essential in the development of commercially successful liquid crystal displays. Further, the low absorption LC materials are useful for some electro-optic modulators in the UV region [6].

In order to understand the alkyl chain length dependence and the agreement among the methods more closely, a graphical representation of number of carbon atoms with transition energy of nPFHEB molecules has been shown in Fig. 5. Evidently, all the methods show a good agreement in exhibiting the transition energy values with increment of number of carbon atoms. Further, the methods also have a good agreement with the shift of absorption wavelength, and oscillator strength values (Table 2, 3, 4). The tendency of increment/ decrement of these parameters with respect to homologue number are the same in the three methods.

Table 2. The absorption bands (AB), extinction coefficients (EC), Oscillator strength (f), Vertical transition energy (E_V), HOMO (H), LUMO (L) energies, and the band gap ($E_g=E_L-E_H$) of nPFHEB (n=5, 6, and 9) molecules using DFT method

Molecule	Absorption Bands/ nm	EC*	f	E_V/ eV
5PFHEB	**213.48**	0.82	0.40	5.77
	256.84	0.24	0.24	4.83
	290.23	0.01	0.01	4.27
	H = -9.19eV	L = -0.62eV	E_g = 8.57eV	
6PFHEB	**213.47**	0.81	0.39	5.78
	256.25	0.23	0.23	4.84
	290.82	0.004	0.004	4.27
	H = -9.19eV	L = -0.65eV	E_g = 8.54eV	
9PFHEB	**215.82**	0.46	0.42	5.73
	270.90	0.30	0.26	4.58
	294.92	0.01	0.01	4.20
	H = -9.03eV	L = -0.64eV	E_g = 8.39eV	

Bold value represents λ_{max}/ nm   *EC unit: 10^4 dm^3 mol^{-1} cm^{-1}

Table 3. The absorption bands (AB), extinction coefficients (EC), Oscillator strength (f), Vertical transition energy (E_V), HOMO (H), LUMO (L) energies, and the band gap ($E_g=E_L-E_H$) of nPFHEB (n=5, 6, and 9) molecules using CNDO/S method

Molecule	Absorption Bands/ nm	EC*	f	E_V/ eV
5PFHEB	**222.26**	0.34	0.34	5.58
	276.17	0.005	0.005	4.48
	H = -9.64eV	L = -0.91eV	E_g = 8.73eV	
6PFHEB	**221.68**	0.32	0.32	5.59
	274.41	0.01	0.005	4.50
	H = -9.63eV	L = -0.89eV	E_g = 8.74eV	
9PFHEB	**232.81**	0.52	0.52	5.32
	262.69	0.01	0.004	4.73
	H = -9.47eV	L = -1.10eV	E_g = 8.37eV	

Bold value represents λ_{max}/ nm   *EC unit: 10^4 dm^3 mol^{-1} cm^{-1}

Table 4. The absorption bands (AB), extinction coefficients (EC), Oscillator strength (f), Vertical transition energy (E_V), HOMO (H), LUMO (L) energies, and the band gap ($E_g=E_L-E_H$) of nPFHEB (n=5, 6, and 9) molecules using INDO/S method

Molecule	Absorption Bands/ nm	EC*	f	E_V/ eV
5PFHEB	**235.74**	0.52	0.52	5.25
	H = -8.58eV	L = -0.29eV	E_g = 8.29eV	
6PFHEB	**235.15**	0.50	0.50	5.28
	H = -8.58eV	L = -0.26eV	E_g = 8.32eV	
9PFHEB	**247.46**	0.60	0.60	5.01
	H = -8.42eV	L = -0.47eV	E_g = 7.95eV	

Bold value represents λ_{max}/ nm   *EC unit: 10^4 dm^3 mol^{-1} cm^{-1}
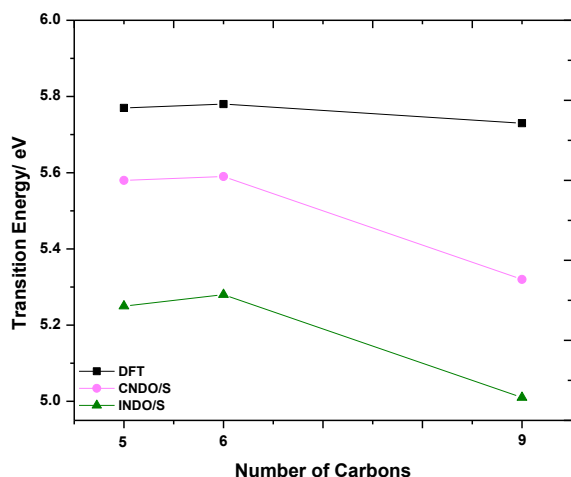
Fig. 5. Variation of transition energy with respect to homologue number of nPFHEB molecules

3.4. Correlation in molecular structure and intensity profiles

The strongest absorption band for all the molecules using the three methods have been found almost in the same range of wavelength (DFT: 5PFHEB: 202.93nm-225.20nm, 6PFHEB: 202.93nm-224.61nm & 9PFHEB: 204.69nm-226.95nm; CNDO/S: 5PFHEB: 208.20nm-243.36nm, 6PFHEB: 208.20nm-242.77nm & 9PFHEB: 212.30nm-253.90nm; INDO/S: 5PFHEB: 217.58nm-256.25nm, 6PFHEB: 215.82nm-258.01nm & 9PFHEB: 223.29nm-270.24nm). This indicates the identical absorption spectrum for all the molecules in UV region due to the similar π-electron structure.

The oscillator strength is a dimensionless quantity that expresses the probability of absorption of electromagnetic radiation in transitions between energy levels of an atom or molecule. It indicates the allowedness of electronic transitions in a molecule, and it is particularly valuable as a method of comparing 'transition strengths' between different types of quantum mechanical systems. Fig. 6 shows a graph has been plotted between wavelength, and oscillator strength to understand the intensity profiles of the compounds based on DFT values. It may be observed from the figure that 5PFHEB molecule exhibits the highest oscillator strength at 212nm, 6PFHEB at 212.10nm, and 9PFHEB at 216.40nm. Further, these molecules exhibit the last intensity peak around 290.30nm, 290.50nm, and 294.90nm respectively. This indicates the much flexibility of 9PFHEB molecule for electronic transitions over a long wavelength region, and high photo sensitivity for this molecule, which may be exploited for optical, electronic applications. The continuous decrease in absorption (Fig. 2, 3, 4), and oscillator strength (Fig. 6) clearly indicates the breakage of aromatic rings with respect to the higher wavelengths, and subsequently loosing the photo sensitivity. This decrease in absorption as a function of increasing UV wavelength has been consistently observed for all the molecules. These two important features of the spectra of these molecules are expected from the correlations in molecular structures. Further, it may be noticed from the figure that in a particular region of

wavelength, the molecules show no absorption. This may be explored for desired applications.
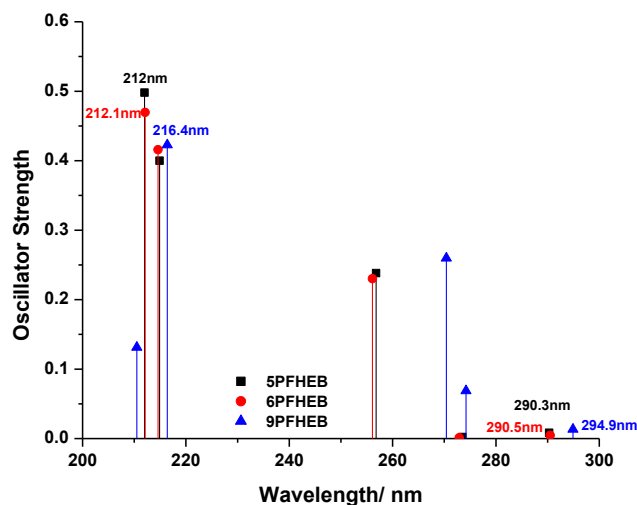
Fig. 6. Wavelength versus oscillator strength of nPFHEB molecules using DFT method

The HOMO, LUMO, and energy gap of the molecules using the three methods have been reported in Table 2, 3, 4. The energy of the HOMO is directly related to the ionization energy, LUMO energy is directly related to the electron affinity. Energy difference between HOMO and LUMO orbital is called as energy gap, which is an important factor for analyzing the stability of the structures. The chemical hardness is a measure for resistance to deformation or change, is very important tool to study the stability of molecular systems, and is also an approximation to the first electron excitation energy. The lowering of energy separation between the HOMO and LUMO clearly explicates the charge transfer interactions taking place within the molecule. The average value of the HOMO and LUMO energies is related to the electro negativity. The negative of the electro negativity is the chemical potential (μ).

A comparison of ionization energy, electron affinity, chemical hardness, electronic chemical potential, Electrophilicity index, and softness of isolated molecules have been made as reported in Table 5. Evidently, all the molecules exhibit good agreement among three methods. The HOMO value of 5PFHEB and 6PFHEB are similar (this may be understood dur to the large correlation between these two structures), and higher to 9PFHEB, due to the longer shift λ_{max} after substitution. However, the energy gap (E_g) shows a preference with increment in end alkyl groups. The increment of alkyl groups in the end chain causes a decrement in optical gap E_g, thereby increasing the conductivity of the molecule. Further, the soft molecule has a small energy band gap, but hard molecule has a large one. Hence, these parameters directly confirm the high flexibility of the molecules. Further, since, the energy gap determines the molecular reactivity such as the ability to absorb light, and to react with other species, a molecule with small gap is expected to have higher reactivity, and a lower stability in photo-physical processes.

Table 5. Calculated values of ionzsation energy I=(-E_H), electron affinity A=(-E_L), electro negativity χ= (I+ A)/2,
chemical hardness η=(I-A)/2, electronic chemical potential μ=(-(I+A)/2, electrophilicity index ω= μ²/η, and
softness S=1/η of nPFHEB (n=5, 6, 9) compounds using TDDFT, CNDO/S, and INDO/S levels

Molecule	Method	I/eV	A/eV	χ/eV	η/eV	μ/eV	ω/eV	S/eV⁻¹
5PFHEB	TDDFT	9.19	0.62	4.90	4.28	-4.90	5.61	0.23
	CNDO/S	9.64	0.91	5.27	5.27	-5.27	6.37	0.23
	INDO/S	8.58	0.29	4.43	4.14	-4.43	4.74	0.24
6PFHEB	TDDFT	9.19	0.65	4.87	4.27	-4.87	5.55	0.23
	CNDO/S	9.63	0.89	5.26	4.37	-5.26	6.33	0.23
	INDO/S	8.58	0.26	4.42	4.16	-4.42	4.70	0.24
9PFHEB	TDDFT	9.03	0.64	4.83	4.19	-4.83	5.57	0.24
	CNDO/S	9.47	1.10	5.28	4.18	-5.28	6.67	0.24
	INDO/S	8.42	0.47	4.44	3.97	-4.44	4.96	0.25
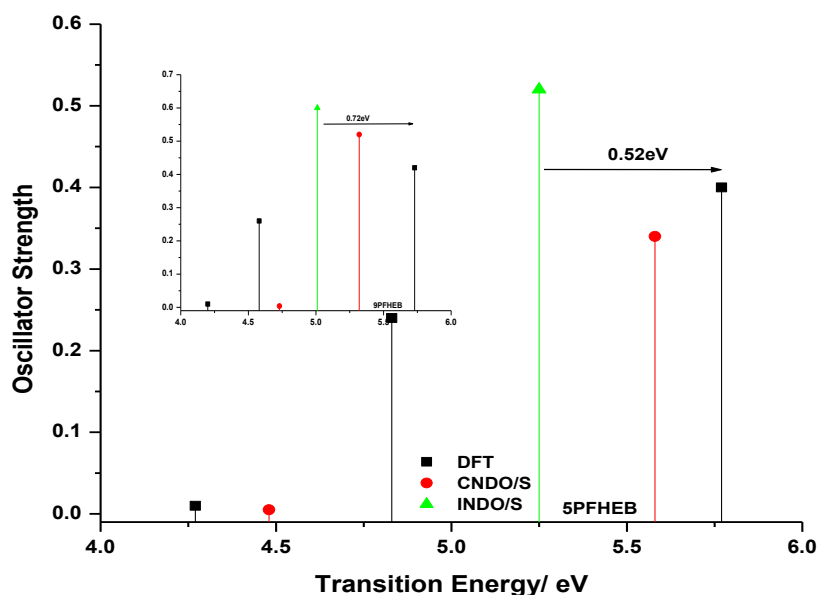
Fig. 7. Transition energy versus oscillator strength of nPFHEB (n=5, 9) molecules

Calculated vertical excitation energies are relatively sensitive to the method employed. This is supported by a collection of results for 5PFHEB and 9PFHEB molecules using the three methods (Fig. 7). It is evident from the Fig. 7 that in case of 5PFHEB, the results from the different methods are within a range of 0.52eV. However, the similar analysis on 6PFHEB and 9PFHEB reveals the results within a range of 0.62eV and 0.72eV respectively. It may be concluded from the above discussion that all the molecules doesn't exhibit excitation energies in a same range, and the increment in homologue number affect the range of the energy values minutely. Further, it is important to note here that in spite of the spread of transition energies, the relative energies between lowest to highest transitions show more consistency among the individual methods.

4. Conclusion

The charge distribution studies estimates the high phase stability for 5PFHEB. Further, the thermal vibration amplitude of the end chain carbon atoms distinctly increases with the increase of chain length. This indicates low packing efficiency for higher homologues. This leads to the drastic decrease in phase stability. This is in agreement with the smectic B-isotropic transition temperature reported by the crystallographer. The comparison of absorption maxima values indicates high photo sensitivity of 9PFHEB. The appearance of strongest absorption band for all molecules in almost the same range of wavelength indicates the identical absorption spectrum in UV region, and the similar π-electron structure. The increment of alkyl groups in the end chain causes a decrement in optical gap E_g, thereby increasing the

conductivity of the molecule. Further, the soft molecule has a small energy band gap, but hard molecule has a large one. Hence, these parameters directly confirm the high flexibility of the molecules. Since, the energy gap determines the molecular reactivity, a molecule with small gap is expected to have higher reactivity, and a lower stability in photo-physical processes.

Acknowledgement

References

[1] M. L. Rahaman, G. Hegde, M. Azazpour, M. M. Yusoff, S. Kumar, J. Fluorine Chem. **156,** 230 (2013).

[2] P. L. Praveen, D. P. Ojha, Mat. Chem. Phys. **135,** 628 (2012).

[3] P. L. Praveen, D. P. Ojha, Mol. Cryst. Liq. Cryst. **571,** 30 (2013).

[4] L. D. Lopes, A. A. Merlo, Mol. Cryst. Liq. Cryst. **612,** 149 (2015).

[5] M. Hird, Chem. Soc. Rev. **36,** 2070 (2007).

[6] S. Ghosh, P. Nayek, S. Kr Roy, T. P. Majumder, R. Dabrowski, Liq. Cryst. **37,** 369 (2010).

[7] J. W. Huh, B. H. Yu, D. M. Shin, T. H. Yoon, Proc. SPIE **9384,** 938417 (2015).

[8] P. L. Praveen, D. P. Ojha, Mol. Cryst. Liq. Cryst. **548,** 209 (2011).

[9] K. Bakhouche, Z. Dhaouadi, S. Lahmar, D. Hammoutene, J. Mol. Model. **21,** 158 (2015).

[10] S. N. Steinmann, C. Corminboeuf, J. Chem. Theo. Computation **8,** 4305 (2012).

[11] R. L. Ellis, G. Kuehnlenz, H. H. Jaffe, Theor. Chim. Acta **26,** 131 (1972).

[12] D. B. Roubaud , J. Kister, L. Bouskasse, J. Metzger, Spect. Lett. **14,** 431 (1981).

[13] P. L. Praveen, D. P. Ojha, J. Mol. Liq. **197,** 106 (2013).

[14] M. Adachi, S. Nakamura, Dyes and Pigments **17,** 287 (1991).

[15] E. Botek, C. Giribet, M. R. D. Azua, R. M. Negri, D. Bernik, J. Phys. Chem. A **112,** 6992 (2008).

[16] K. Hori, M. Maeda, M. Yano, M. Kunugi, Liq. Cryst. **38,** 287 (2011).

[17] C. R. Bhattacharjee, G. Das, P. Mondal, S. K. Prasad, D. S. S. Rao, Inorg. Chem. Commu. **14,** 606 (2011).

[18] P. Hohenberg, W. Kohn, Phys. Rev. **136,** B864 (1965).

[19] W. Kohn, L. J. Sham, Phys. Rev. **140,** A1133 (1965).

[20] R. O. Jones, O. Gunnarsson, Rev. Mod. Phys. **61,** 689 (1989).

[21] P. L. Praveen, D. S. Ramakrishna, Int. Adv. Res. J. Sci. Engg. Technol. **2,** 92 (2015).

[22] M. T. Sims, L. C. Abbott, S. J. Cowling, J. W. Goodby, J. N. Moore, Chemistry: A Eur. J. **21,** 10123 (2015).

[23] F. A. Neese, J. Chem. Phys. **119,** 9428 (2003).

[24] M. J. Hervai, G. A. Webb, Org. Mag. Res. **13,** 116 (1980).

[25] H. Suzuki, Electronic Absorption Spectra and Geometry of Organic Molecules: An Application of Molecular Orbital Theory Academic Press INC. New York (1967).

[*]Corresponding author: plpraveen_phy@vssut.ac.in